Published in final edited form as:
*Environ Sci Technol*. 2010 April 15; 44(8): 3073–3078. doi:10.1021/es100787m.

# Phosphate Removal by Anion Binding on Functionalized Nanoporous Sorbents

**Wilaiwan Chouyyok**,
Pacific Northwest National Laboratory Richland, WA 99352

**Robert J. Wiacek**,
Pacific Northwest National Laboratory Richland, WA 99352

**Kanda Pattamakomsan**,
Pacific Northwest National Laboratory Richland, WA 99352

**Thanapon Sangvanich**,
Department of Biomedical Engineering, OHSU School of Medicine, Portland, OR 97239

**Rafal M. Grudzien**,
Pacific Northwest National Laboratory Richland, WA 99352

**Glen E. Fryxell***, and
Pacific Northwest National Laboratory Richland, WA 99352

**Wassana Yantasee***
Department of Biomedical Engineering, OHSU School of Medicine, Portland, OR 97239

## Abstract

Phosphate was captured from aqueous solutions by cationic metal-EDA complexes anchored inside mesoporous silica MCM-41 supports (Cu(II)-EDA-SAMMS and Fe(III)-EDA-SAMMS). Fe-EDA-SAMMS was more effective at capturing phosphate than the Cu-EDA-SAMMS and was further studied for matrix effects (e.g., pH, ionic strength, and competing anions) and sorption performance (e.g., capacity and rate). The adsorption of phosphate was highly pH dependent; it increased with increasing pH from 1.0 to 6.5, and decreased above pH 6.5. The adsorption was affected by high ionic strength (0.1 M of NaCl). In the presence of 1000-fold molar excess of chloride and nitrate anions, phosphate removal by Fe-EDA-SAMMS was not affected. Slight, moderate and large impacts were seen with bicarbonate, sulfate and citrate anions, respectively. The phosphate adsorption data on Fe-EDA-SAMMS agreed well with the Langmuir model with the estimated maximum capacity of 43.3 mg/g. The material displayed rapid sorption rate (99% of phosphate removal within 1 min) and lowering the phosphate content to ~ 10 μg/L of phosphorus, which is lower than the EPA's established freshwater contaminant level for phosphorous (20 μg/L).

## Introduction

Excess phosphate in bodies of water can lead to significant eutrophication and water quality problems. Excessive phosphate results in the growth of aquatic plants, including harmful algal blooms, as well as depletion of dissolved oxygen that subsequently results in the decline of aquatic life. To control excessive growth of algae and other nuisance plants in natural water, the US-EPA has an established a maximum contaminant level for phosphorus to be < 20 μg/L in rivers and streams [1] and in lakes and reservoirs [2] during summer growing season or

*(509)375-3856 (office), (509)375-2186 (fax), glen.fryxell@pnl.gov. *503-418-9306 (office), 503-418-9311 (fax), yantasee@ohsu.edu.

< 2 mg/L in estuarine and coastal marine waters [3]. The amount of phosphate pollution has been increasing as a result of wastes generated from industrial, agricultural and household sources. Therefore, to achieve levels below the limits set by EPA, various techniques, including chemical precipitation, biological treatment, and adsorption, have been used and studied for phosphate removal [4]. While chemical precipitation is better suited at the higher phosphate concentrations encountered in some industrial waste streams, the development of adsorbents for phosphate capture has been most widely studied due to their high efficiency at low phosphate concentrations [5–7]. Adsorption provides faster phosphate removal rate than does biological-based phosphate treatment. Therefore, a variety of adsorbents have been developed recently and evaluated for phosphate removal, including slag [8,9], red mud [10], palygorskite [11], iron based components [5,12], zirconium [13–15], coal fly ash [16,17], crab shells[18], lithium [19], and MgMn-layered double hydroxides [20]. Among these materials, lanthanum (III) plays an important role in the field of phosphate removal [6,7,21–23] because it is a moderately hard trivalent Lewis acid, and has a high affinity for phosphate, which is a hard base [23]. The maximum adsorption capacity for those La(III) based sorbents for phosphate was reported to be about 25 mg phosphorus/g [6] but took as long as 24 hours to achieve.

Self-assembled monolayers on mesoporous supports (SAMMS®[24]) have been developed at PNNL over the last decade for removal of heavy metals and radionuclides from aqueous systems[25]. Their extremely high surface areas and dense, ordered ligand arrays have provided high loading capacity, strong ligand binding stability, and rapid binding rate for a variety of metal chelations [26–29]. It has been reported that cationic Cu(II) and Fe(III)-EDA complexes bound to the pore walls inside mesoporous silica are capable of binding toxic anions like arsenate and chromate [27,30–32]. Additionally, Yokoi et al.[31] reported that phosphate could compete with oxyanions to bind with a Fe(III) complex, suggesting that perhaps the metal-complexes might also be effective for phosphate binding.

Therefore, we set out to study how effectively metallated EDA-SAMMS were able to capture phosphate anion from buffered aqueous media in batch contact experiments. These studies were tailored to study the effect of pH, ionic strength and coexisting anions on phosphate capture, as well as a determination of the adsorption isotherm and phosphate sorption kinetics. This manuscript summarizes these results.

## Experimental Procedures

### Sorbent

Two sorbent materials were used; Cu-EDA-SAMMS and Fe-EDA-SAMMS. The details of the synthesis of Cu-EDA-SAMMS were described in our previous work [27]. In short, the pre-hydrated MCM-41 (the MCM-41 used had a specific surface area of 880 $m^2$/g, an average pore diameter of ~30 Å, and a pore volume of 1.29 cc/g) [33–36] was treated with ethylenediamine (EDA) terminated silane [1-(2 aminoethyl)- 3-aminopropyl]trimethoxysilane] in refluxing toluene to produce EDA-SAMMS. Incorporation of the Cu(II) ions was accomplished by stirring the EDA-SAMMS in an aqueous solution of a slight excess of $CuCl_2$ for a few hours to produce the Carolina blue Cu-EDA-SAMMS. The metalized adduct was collected by filtration, washed with water, then 2-propanol, and air-dried. Fe-EDA-SAMMS was prepared by a similar method, using a slight excess of $FeCl_3$ in place of $CuCl_2$.

Elemental analysis (Galbraith Laboratories) of Cu-EDA-SAMMS revealed a mass composition of 14.41% C, 3.28% H, 5.31% N, and 3.35% Cu. Similar analysis for Fe-EDA-SAMMS revealed a composition of 11.75% C, 3.21% H, 4.81% N, and 4.62% Fe.

Fourier transform infrared (FTIR) spectroscopic analysis of Cu-EDA-SAMMS (Nicolet Magna IR 750 Spectrometer) revealed a broad band from ~3700 $cm^{-1}$ ranging down to ~2600

$cm^{-1}$ (centered at ~3300 $cm^{-1}$) consistent with an N-H stretch of a metal coordinated amine. At 2960 $cm^{-1}$ and 2910 $cm^{-1}$ were observed the C–H stretching bands associated with the propyl tether and the EDA ligands. A moderately strong band was observed at 1570 $cm^{-1}$ consistent with the N-H bending vibration of a metallated amine. A weak shoulder was observed at 1470 $cm^{-1}$, and was assigned to the scissoring band of the methylene groups. A relatively weak band was also observed at 1420 $cm^{-1}$, tentatively assigned to N-H bending. A broad band ranging from ~1300 $cm^{-1}$ to ~900 $cm^{-1}$ (strongest absorption at 1110 $cm^{-1}$) obliterated much of the fingerprint region of the spectrum and is assigned to the Si-O stretching vibration. A moderately strong peak was observed at 802 $cm^{-1}$, and is assigned to the N-H wagging vibration.

Similar FTIR analysis of Fe-EDA-SAMMS revealed a broad strong band ranging from ~3700 $cm^{-1}$ to ~2600 $cm^{-1}$ (strongest absorption at 3440 $cm^{-1}$) consistent with a metallated N-H stretching vibration. C–H stretching bands were observed at 2970 $cm^{-1}$ and 2910 $cm^{-1}$. A fairly strong band was observed at 1660 $cm^{-1}$, and is assigned to the N-H bending vibration of a metallated amine. A relatively weak band was found at 1470 $cm^{-1}$ and is assigned to the scissoring band of the $CH_2$ groups. A strong, broad band ranging from ~1340 $cm^{-1}$ down to ~900 $cm^{-1}$ (strongest absorbance at 1110 $cm^{-1}$) is assigned to the Si-O stretching vibrations. A moderately strong band at 806 $cm^{-1}$ is attributed to the N-H wagging vibration.

Brunauer-Emmett-Teller (BET) surface area analysis of Cu-EDA-SAMMS revealed a surface area of 117 $m^2/g$ and a pore volume of 0.58 cc/g. BET surface area analysis of Fe-EDA-SAMMS revealed a surface area of 169 $m^2/g$ and a pore volume of 0.68 cc/g. In both cases the average pore diameter was found to be less than 20Å.

## $K_d$ measurements

The distribution coefficients of phosphate in deionized distilled (DI) water were measured in batch experiment with ~ 2 ppm of initial phosphate ($KH_2PO_4$) concentration. A 0.01 g weight of sorbent and 10 mL volume (liquid-to-solid ratio (L/S), of 1000 mL/g) of the test solution was shaken in a polypropylene bottle at a speed of 200 rpm for 2 hrs at room temperature. After 2 hrs, the solution was removed by filtering thru 0.45-μm syringe Nylon-membrane filters and the filtrate was kept in 2 vol. % $HNO_3$ prior to metal analysis. The concentrations in the control (no sorbent) and the test solutions (after being contacted with a sorbent material) were analyzed using an inductively coupled plasma-mass spectrometer (ICP-MS, Agilent 7500ce, Agilent Technologies, CA). All batch experiments were performed in triplicates and the averaged values were reported.

## pH and ionic strength studies

The effects of solution pH and ionic strength on phosphate removal were measured in the same fashion with the $K_d$ measurements, solutions containing ~2 ppm of phosphate and a known concentration of NaCl (from 0.001–0.1 M) were adjusted with HCl or NaOH to the desired pH values. After the batch contact with a sorbent material, the equilibrium pH was measured and the solution was filtered. The filtrate was analyzed for P using an ICP-MS. The percent phosphate removal was calculated as Equation 1:

$$phosphate\ removal = 100 \times \frac{(C_0 - C_f)}{C_0} \quad (1)$$

where $C_o$ and $C_f$ are the initial and final concentrations of the phosphate, respectively

### Coexisting anions

The effect of common coexisting anions in waste water including chloride, nitrate, bicarbonate, sulfate, and citrate on the adsorption of phosphate on Fe-EDA-SAMMS was investigated in the same fashion with the $K_d$ measurement, except that 0.1 M of chloride, nitrate, bicarbonate, sulfate, and citrate (all in sodium form) were added to solutions containing ~1 ppm of phosphate.

### Sorption capacity

The sorption capacity of Fe-EDA-SAMMS for phosphate was measured in the same fashion with the $K_d$ measurements, except that the initial phosphate concentration was varied until the maximum sorption capacity was obtained. This was accomplished by using a large molar excess of phosphate to the binding sites on the sorbent material (e.g., 0.02 to 18.53 mg/L of phosphate at liquid-to-solid ratio of 10,000 mL/g).

### Sorption kinetics

The kinetics of metal sorption was performed on Fe-EDA-SAMMS in the same fashion with the $K_d$ measurements, except that the sample volume was increased to 50 mL to minimize the change in liquid-to-solid ratio due to the frequent samplings (e.g., 1 mL each of well-mixed aliquot at 1, 2, 3, 5, 10, 30, 60 min, 2, 4, 8, and 24 hr). The same solution without contacting with Fe-EDA-SAMMS served as zero time point.

## Results and Discussion

Functionalized mesoporous silica materials containing cationic transition metal complexes built around Cu(II) and Fe(III) ions have demonstrated excellent anion exchange behavior for arsenate and chromate [27,30–32]. In this work, we investigated the Fe(III) ethylenediamine on mesoporous silica (Fe-EDA-SAMMS) and copper ethylenediamine on mesoporous silica (Cu-EDA-SAMMS) for the capture of phosphate anions (as $H_2PO_4^{-1}$ and $HPO_4^{-2}$). Synthesis of these sorbents was carried out by exposing EDA-SAMMS to a modest excess of the appropriate metal chloride salt in water. We wanted to get the highest metal salt loading possible in order to evaluate the efficacy of these nanoporous anion exchange materials for capturing phosphate anion, and therefore we did not look at lesser metal concentrations in these sorbents.

Elemental analysis of the Cu-EDA-SAMMS and Fe-EDA-SAMMS revealed that they contained approximately 0.53 mmoles of Cu and 0.83 mmoles of Fe per gram of sorbent, respectively. In each case, the sorbent was found to contain 1.8 (±0.1) mmoles of EDA ligand per gram of sorbent, indicating a 1:3.4 stoichiometry for the Cu-EDA complex (i.e. not all the EDA ligand was metallated). While this is consistent with the originally proposed Cu $(EDA)_3$ complex [26], it is more likely that the primary species is a $Cu(EDA)_2X$ complex, as characterized in detail by Yoshitake [37] (shown in Figure 1). In any event, there appears to be “leftover” EDA that is not complexed to a Cu(II) ion when this material is prepared under these conditions. The Fe-EDA-SAMMS was found to have a 1:2.2 stoichiometry for the Fe-EDA complex, which presumably represents a mixture of the 1:2 and 1:3 complexes (both of which are shown in Figure 1).

Characterization of these materials by FTIR revealed the bands expected for an N-H bound to a Lewis acid metal center (broad N-H stretch from ~3700 $cm^{-1}$ to ~2600 $cm^{-1}$, an N-H bending vibration at ~1600 $cm^{-1}$, and an N-H wag at ~805 $cm^{-1}$), as well as the expected C–H stretches associated with the propyl tether and EDA ligand (2970 $cm^{-1}$ to 2910 $cm^{-1}$), and the intense broad band associated with the Si-O stretches (around 1100 $cm^{-1}$) of the MCM-41 support.

The MCM-41 that we started with had a specific surface area of 880 $m^2$/g, an average pore diameter of 30Å, and a pore volume of 1.29 cc.g. Installation of the metallated EDA monolayers reduces all three of these values significantly, as would be expected, both from the addition of significant mass, as well as the reduction in absolute surface area due to the significant volume occupied by the metallated EDA monolayer within the pore. The Cu-EDA-SAMMS was found to have a specific surface area of 117 $m^2$/g (as measured by BET) and a pore volume of 0.58 cc/g. Fe-EDA-SAMMS revealed a surface area of 169 $m^2$/g and a pore volume of 0.68 cc/g. In both cases the average pore diameter was found to be less than 20Å. These observations are all consistent with the installation of a monolayer coating throughout the nanoporous matrix, containing $M(EDA)_n$ complexes, adding mass and consuming pore volume.

The phosphate sorption performance of Cu-EDA-SAMMS and Fe-EDA-SAMMS was evaluated in term of the distribution coefficient ($K_d$, mL/g), which is simply a mass-weighted partition coefficient between solid phase and liquid supernatant phase as shown in Equation 2:

$$K_d = \frac{(C_0 - C_f)}{C_f} \frac{V}{M} \tag{2}$$

where $C_o$ and $C_f$ are the initial and final concentrations of the analyte, respectively (at equilibrium), V is the volume of solution, and M is the mass of sorbent used. These initial scoping measurements were carried out in deionized water, with an initial phosphate concentration of ~2 ppm (in the form of $KH_2PO_4$). The liquid-to-solid ratio was 1000 mL/g. These comparative results are summarized in Table 1. According to Pearson's hard soft acid base theory [38], Fe (III) ion is a "harder" Lewis acid than is Cu(II) ion. As a result, Fe(III) is able to bind phosphate (a hard base) more strongly than Cu(II) ion (similar results were obtained by Yoshitake and co-workers for arsenate anion [31]). In addition, Fe-EDA-SAMMS leached less metal ligand and silica than did Cu-EDA-SAMMS. Therefore, Fe-EDA-SAMMS was chosen for further evaluations for the matrix effects (pH, ionic strength, and other anions) as well as the phosphate sorption capacity and rate.

## Adsorption Isotherm

In order to determine the maximum adsorption capacity of Fe-EDA-SAMMS for phosphate, the adsorption isotherms were measured in DI water containing different concentrations of phosphate (pH ~5) and at liquid-to-solid ratio of 10,000 mL/g. The adsorption isotherm data fit the Langmuir adsorption model well, as shown in Figure 2 ($R^2 > 0.99$), indicating the adsorption of phosphate anions is taking place in a monolayer fashion. The adsorption capacity of phosphate increased with increasing equilibrium phosphate concentration and reached a maximum once the equilibrium phosphate concentration approaching 5 ppm, indicating the adsorption sites were saturated. The maximum adsorption capacity of phosphate was 43.3 mg (0.46 mmol) per g of Fe-EDA-SAMMS. At a functional loading of 0.83 mmole Fe(III) per gram of sorbent, it appears that a little over half of the Fe(III) binding sites have been used to bind the phosphate anion (the fact that in this pH range we are dealing with the phosphate monoanion argues against the possibility of a phosphate dianion bridging between two Fe centers). This maximum phosphate capacity is significantly higher than those reported for sorbents like La doped vesuvianite (4.0 mg/g) [21], Fe oxide tailing (21.5 mg/g) [40], Fe(III)/Cr(III) hydroxide (6.5 mg/g) [12], and MgMn-layered double hydroxides (22.3 mg/g) [20], and comparable to sorbents like La/Al pillared montmorillonite (40.0 mg/g) [22], Fe-Mn binary oxide adsorbent (36.0 mg/g) [5], and commercial zirconium ferrite (39.8 mg/g) [14]. For La (III) mesoporous silica, $LaPO_4$ formed during the adsorption was suspected of blocking the pores of La-based mesoporous silica [7].

Successful binding of phosphate anion with these materials raises the question of the binding mechanism by which phosphate anion is being bound – is it a simple ion exchange process (i.e. no direct bond formation between the metal center and the anion), or is it a direct coordination process (where there is a bond formed between the anion and the metal center)? Detailed XAFS studies have shown that Cu-EDA-SAMMS binds oxometallate anions like chromate and arsenate by displacing an EDA ligand from the Cu(EDA) complex and forming a monodentate bond between the anion and the Cu center [39]. The ability of the anion to participate in this displacement reaction has been correlated to its basicity [38]. Similar XAFS studies for the Fe-EDA complex (also in mesoporous silica) binding arsentate, chromate, selenate, and molybdate anions found direct evidence of the oxoanion is bound directly to the metal center (in fact, in some cases, the authors found evidence of two arsenate anions binding to a single Fe center!) [37]. Based on these precedents, and the basicity of phosphate monoanion ($pK_b$ of 11.9), we postulate that the phosphate anion is directly bound to the Fe(III) ion of the $Fe(EDA)_n$ complex in these sorbent materials, most likely in a monodentate fashion. This raises an interesting observation – the Fe/EDA ratio observed in these materials was 1:2.2, consistent with a mixture of 1:2 and 1:3 complexes (as discussed earlier, see Figure 1), with the 1:2 complex being present at slightly higher levels. Given that only a little over half of the Fe sites are used in binding the phosphate monoanion, this suggests that only the $Fe(EDA)_2X_2$ sites enter into this binding process (see Figure 1), and that the phosphate monoanion is not sufficiently basic to displace the EDA ligand from the $Fe(EDA)_3$ complex. If phosphate binding were taking place through simple ion exchange, then either the $Fe(EDA)_2X_2$ or $Fe(EDA)_3$ complexes should be able to effectively bind the phosphate anion, but if only binding to the $Fe(EDA)_2X_2$ complex is taking place, then that is most consistent with displacement of X and formation of a direct Fe-phosphate bond.

## The effect of pH and ionic strength

The pH of solution has an impact on the speciation of the phosphate ions in solution. At pHs lower than 2.15, the predominant species is the neutral $H_3PO_4$. Between pHs of 2.15–7.20, the predominant species is $H_2PO_4^-$, while at pHs of 7.20–12.33 the main species is $HPO_4^{2-}$ [41]. Additionally, natural waters always contain various anions, and these coexisting ions may affect or compete with phosphate anions for the binding sites of sorbent materials. In order to assess the influence of pH and ionic strength on phosphate removal by Fe-EDA-SAMMS, the batch adsorption were investigated in solutions containing ~2 ppm of phosphate and NaCl at varied concentrations (0.001 M–0.1 M) over the pH range of 1.0 to 11.5. The results are summarized in Figure 3. Phosphate removal increased with increasing pH from 1.0 to 6.5, and then dropped sharply as pH increased from 6.5 to 11.5. At low ionic strength (0.001 – 0.01 M NaCl), the maximum removal of > 98% was achieved from pH 2.5 to 6.5, while at higher ionic strength (0.1 M NaCl), the maximum phosphate removal of > 85% was achieved from pH 5.3 to 6.2. Interestingly, Fe-EDA-SAMMS was able to capture 40–50% of phosphate at pH 1, where the neutral $H_3PO_4$ species was predominant. One possible explanation might be the protonation of the EDA ligands and anion exchange at the newly formed ammonium ion. Support for this hypothesis is found in Figure 4, where Fe is seen to leach out of the sorbent at low pH (note that no significant Si leaching was observed, indicating that the sorbent backbone or monolayer is not breaking down). It appears that this ammonium ion exchange site is not as effective as the Fe-EDA complex and the phosphate binding capacity is markedly lower at pH of 1.0 than it is at a pH of 5.0–6.0. At higher pH (> 6.5), a significant drop in phosphate removal was observed, suggesting that hydroxide anions may be competing with phosphate anions to bind with the binding sites on Fe-EDA-SAMMS [8,14,15]. Likewise, the binding of arsenate and chromate anions at Cu-EDA-SAMMS was found to be a function of the $pK_b$ of the anion [42]. Clearly, the pH of the solution plays an important role on the adsorption of phosphate similar to a number of reports using various sorbents (that bind phosphate more effectively under acidic conditions than alkaline conditions [5–10,12,15,23,

43]). In contrast, there are relatively few reports [13,14,21] that found no significant effect on phosphate removal as pH changed from 2 to 10. Nevertheless, the results show that Fe-EDA-SAMMS would be very effective at removing phosphate in most wastes and natural waters having pH between 2.5 to 6.5 and ionic strength lower than 0.1 M.

### Effect of coexisting anions

Natural waters and waste waters normally contain coexisting ions, which could potentially interfere in the binding of phosphate. Thus, the competitive sorption of the coexisting anions, including chloride, nitrate, bicarbonate, sulfate, and citrate, was studied in DI water containing ~1 ppm of phosphate and 0.01 M of the competing anions (equivalent to 1000-fold molar excess of the phosphate). The results shown in Table 2 demonstrate that there was only small interference for the phosphate adsorption by the presence of 0.01 M chloride and nitrate anions. Phosphate adsorption by Fe-EDA SAMMS was inhibited modestly in the presence of bicarbonate and sulfate, , while chelating citrate anion strongly impacted the phosphate binding. This trend agrees with the previous report that metallated-EDA-SAMMS (e.g., Cu-EDA-SAMMS) binds more basic anions more strongly than the less basic anions[42]. In addition, Yoshitake found that arsenate binding by Fe-EDA was only slightly suppressed by chloride and sulfate, but Cu-EDA was substantially impacted by both chloride and sulfate, revealing an important degree of chemical selectivity of the Fe-based sorbent over the Cu-based sorbent [37]. Competing anion effects on phosphate removal have also been found on other types of adsorbents [8,14]. However, for La/Al pillared montmorillonite, it was reported that phosphate removal was more strongly affected by chloride ion than by nitrate and sulfate anions[22]. In light of these observations, it appears that Fe-EDA-SAMMS is well-suited for removal of phosphate in the presence of chloride and nitrate anions (which are commonly found in natural waters and a variety of common wastestreams).

### Adsorption kinetics

Adsorption kinetics plays an important role in the efficiency and field-deployment costs of a sorbent [26]. Therefore, the adsorption kinetics of Fe-EDA-SAMMS for binding phosphate was studied under the same conditions as our pH studies (~2.8 ppm of phosphate and L/S of 1000 mL/g). Figure 5 shows the reduction of phosphate concentration in the solution as a function of contact time. The concentration was reduced from 2.82 ppm to 0.035 ppm (equivalent to ~ 99% reduction) within 1 min and remained relatively constant over the 24 hours of contact time. The reaction reached equilibrium within ~1 min. Rapid phosphate sorption was facilitated by the rigid and open pore structure of the mesoporous silica, allowing easy access of phosphate anions to the binding sites. Fast sorption kinetics are highly beneficial for the rapid through-put of the phosphate-containing process stream. In comparison, the Fe-EDA-SAMMS offers much faster phosphate uptake rate than the widely studied La [6,7,21, 22] and Fe-based sorbents [5,12], which normally take several hours to reach sorption equilibrium.

## Acknowledgments

This work was supported by the National Institute of Allergy and Infectious Disease (NIAID), grant# R01 AI074064, the National Institute of Environmental Health Sciences (NIEHS), grant# R21 ES015620, and DOE Laboratory Directed Research and Development funding. A portion of research was performed using EMSL, a national scientific user facility sponsored by the Department of Energy's Office of Biological and Environmental Research and located at Pacific Northwest National Laboratory. Pacific Northwest National Laboratory is operated for the U.S. Department of Energy by Battelle under contract DE-AC06-67RLO 1830.

## Literature Cited


1. Nutrient criteria technical guidance manual: rivers and streams. Washington, DC: Office of Science and Techlonogy, U.S. EPA; 2000. EPA-822B-00-002
2. Nutrient criteria technical guidance manual: lakes and reservoirs. Washington, DC: Office of Science and Technology, U.S. EPA; 2000. EPA-822-B00-001
3. Nutrient criteria technical guidance manual: estuarine and coastal marine waters. Office of Water, U.S. EPA; 2001. EPA-822-B-01-003
4. Morse GK, Brett SW, Guy JA, Lester JN. Review: Phosphorus removal and recovery technologies. Sci. Total Environ 1998;212(1):69–81.
5. Zhang G, Liu H, Liu R, Qu J. Removal of phosphate from water by a Fe-Mn binary oxide adsorbent. J. Colloid Interface Sci 2009;335(2):168–174. [PubMed: 19406416]
6. Ning P, Bart H–J, Li B, Lu X, Zhang Y. Phosphate removal from wastewater by model-La(III) zeolite adsorbents. J. Environ. Sci 2008;20(6):670–674.
7. Ou E, Zhou J, Mao S, Wang J, Xia F, Min L. Highly efficient removal of phosphate by lanthanum-doped mesoporous $SiO_2$*Colloids and Surfaces A: Physicochem*. Eng. Aspects 2007;308(1–3):47–53.
8. Xue Y, Hou H, Zhu S. Characteristics and mechanisms of phosphate adsorption onto basic oxygen furnace slag. J. Hazard. Mater 2009;162(2–3):973–980. [PubMed: 18614283]
9. Xiong J, He Z, Mahmood Q, Liu D, Yang X, Islam E. Phosphate removal from solution using steel slag through magnetic separation. J. Hazard. Mater 2008;152(1):211–215. [PubMed: 17703877]
10. Huang W, Wang S, Zhu Z, Li L, Yao X, Rudolph V, Haghseresht F. Phosphate removal from wastewater using red mud. J. Hazard. Mater 2008;158(1):35–42. [PubMed: 18314264]
11. Gan F, Zhou J, Wang H, Du C, Chen X. Removal of phosphate from aqueous solution by thermally treated natural palygorskite. Water Res 2009;43(11):2907–2915. [PubMed: 19447464]
12. Namasivayam C, Prathap K. Recycling Fe(III)/Cr(III) hydroxide, an industrial solid waste for the removal of phosphate from water. J. Hazard. Mater 2005;123(1–3):127–134. [PubMed: 15955623]
13. Yeon K-H, Park H, Lee S-H, Park Y-M, Lee S-H, Iwamoto M. Zirconium mesostructures immobilized in calcium alginate for phosphate removal. Korean J. Chem. Eng 2008;25(5):1040–1046.
14. Biswas BK, Inoue K, Ghimire KN, Harada H, Ohto K, Kawakita H. Removal and recovery of phosphorus from water by means of adsorption onto orange waste gel loaded with zirconium. Bioresour. Technol 2008;99(18):8685–8690. [PubMed: 18524574]
15. Liu H, Sun X, Yin C, Hu C. Removal of phosphate by mesoporous ZrO2. J. Hazard. Mater 2008;151 (2–3):616–622. [PubMed: 17658689]
16. Guan Q, Hu X, Wu D, Shang X, Ye C, Kong H. Phosphate removal in marine electrolytes by zeolite synthesized from coal fly ash. Fuel 2009;88(9):1643–1649.
17. Pengthamkeerati P, Satapanajaru T, Chularuengoaksorn P. Chemical modification of coal fly ash for the removal of phosphate from aqueous solution. Fuel 2008;87(12):2469–2476.
18. Jeon DJ, Yeom SH. Recycling wasted biomaterial, crab shells, as an adsorbent for the removal of high concentration of phosphate. Bioresour. Technol 2009;100(9):2646–2649. [PubMed: 19144514]
19. Wang S-L, Cheng C–Y, Tzou Y-M, Liaw R-B, Chang T–W, Chen J–H. Phosphate removal from water using lithium intercalated gibbsite. J. Hazard. Mater 2007;147(1–2):205–212. [PubMed: 17240056]
20. Chitrakar R, Tezuka S, Sonoda A, Sakane K, Ooi K, Hirotsu T. Adsorption of phosphate from seawater on calcined MgMn-layered double hydroxides. J. Colloid Interface Sci 2005;290(1):45–51. [PubMed: 15925378]
21. Li H, Ru J, Yin W, Liu X, Wang J, Zhang W. Removal of phosphate from polluted water by lanthanum doped vesuvianite. J. Hazard. Mater 2009;168(1):326–330. [PubMed: 19297092]
22. Tian S, Jiang P, Ning P, Su Y. Enhanced adsorption removal of phosphate from water by mixed lanthanum/aluminum pillared montmorillonite. Chem. Eng. J 2009;151(1–3):141–148.
23. Wu RSS, Lam KH, Lee JMN, Lau TC. Removal of phosphate from water by a highly selective La (III)-chelex resin. Chemosphere 2007;69(2):289–294. [PubMed: 17531289]
24. SAMMS is a registered trademark of Steward Advanced Materials.

25. Fryxell GE, Mattigod SV, Lin Y, Wu H, Fiskum S, Parker K, Zheng F, Yantasee W, Zemanian TS, Addleman RS, Liu J, Kemner K, Kelly S, Feng X. Design and synthesis of self-assembled monolayers on mesoporous supports (SAMMS): The importance of ligand posture in functional nanomaterials. J. Mater. Chem 2007;17(28):2863–2874.
26. Lin Y, Fryxell GE, Wu H, Engelhard M. Selective sorption of cesium using self-assembled monolayers on mesoporous supports. Environ. Sci. Technol 2001;35(19):3962–3966. [PubMed: 11642461]
27. Fryxell GE, Liu J, Hauser TA, Nie Z, Ferris KF, Mattigod S, Gong M, Hallen RT. Design and synthesis of selective mesoporous anion traps. Chem. Mater 1999;11(8):2148–2154.
28. Yantasee W, Fryxell GE, Addleman RS, Wiacek RJ, Koonsiripaiboon V, Pattamakomsan K, Sukwarotwat V, Xu J, Raymond KN. Selective removal of lanthanides from natural waters, acidic streams and dialysate. J. Hazard. Mater. in press.
29. Lin Y, Fiskum SK, Yantasee W, Wu H, Mattigod SV, Vorpagel E, Fryxell GE, Raymond KN, Xu J. Incorporation of Hydroxypyridinone Ligands into Self-Assembled Monolayers on Mesoporous Supports for Selective Actinide Sequestration. Environ. Sci. Technol 2005;39(5):1332–1337. [PubMed: 15787374]
30. Yokoi T, Tatsumi T, Yoshitake H. Selective selenate adsorption on cationated amino-functionalized MCM-41. Bull. Chem. Soc. Jpn 2003;76(11):2225–2232.
31. Yokoi T, Tatsumi T, Yoshitake H. Fe3+ coordinated to amino-functionalized MCM-41: an adsorbent for the toxic oxyanions with high capacity, resistibility to inhibiting anions, and reusability after a simple treatment. J. Colloid Interface Sci 2004;274(2):451–457. [PubMed: 15144816]
32. Yoshitake H, Yokoi T, Tatsumi T. Adsorption Behavior of Arsenate at Transition Metal Cations Captured by Amino-Functionalized Mesoporous Silicas. Chem. Mater 2003;15(8):1713–1721.
33. Beck JS, Vartuli JC, Roth WJ, Leonowicz ME, Kresge CT, Schmitt KD, Chu CTW, Olson DH, Sheppard EW. A new family of mesoporous molecular sieves prepared with liquid crystal templates. J. Am. Chem. Soc 1992;114(27):10834–10843.
34. Kresge CT, Leonowicz ME, Roth WJ, Vartuli JC, Beck JS. Ordered mesoporous molecular sieves synthesized by a liquid-crystal template mechanism. Nature 1992;359(6397):710–712.
35. Feng X, Fryxell GE, Wang L-Q, Kim AY, Liu J, Kemner KM. Functionalized Monolayers on Ordered Mesoporous Supports. Science 1997;276(5314):923–926.
36. Liu J, Feng X, Fryxell GE, Wang LQ, Kim AY, Gong M. Hybrid mesoporous materials with functionalized monolayers. Adv. Mater 1998;10:161–165.
37. Yoshitake, H. Functionalization of Periodic Mesoporous Silica and its Application to the Adsorption of Toxic Anions. In: Fryxell, GE.; Cao, G., editors. Environmental Applications of Nanomaterials: Synthesis, Sorbents and Sensors. Singapore: Imperial College Press; 2007. p. 241-274.
38. Pearson RG. Hard and Soft Acids and Bases. J. Am. Chem. Soc 1963;85(22):3533–3539.
39. Kelly SD, Kemner KM, Fryxell GE, Liu J, Mattigod SV, Ferris KF. X-Ray-Absorption Fine-Structure Spectroscopy Study of the Interactions between Contaminant Tetrahedral Anions and Self-Assembled Monolayers on Mesoporous Supports. J. Phys. Chem. B 2001;105(27):6337–6346.
40. Zeng L, Li X, Liu J. Adsorptive removal of phosphate from aqueous solutions using iron oxide tailings. Water Res 2004;38(5):1318–1326. [PubMed: 14975665]
41. Perrin, DD.; Dempsey, B. Buffers for pH and metal ion control Chapman and Hall. London: 1974.
42. Mattigod SV, Fryxell GE, Parker KE. Anion binding in self-assembled monolayers in mesoporous supports (SAMMS). Inorg. Chem. Commun 2007;10(6):646–648.
43. Abou Taleb MF, Mahmoud GA, Elsigeny SM, Hegazy E-SA. Adsorption and desorption of phosphate and nitrate ions using quaternary (polypropylene-g-N,N-dimethylamino ethylmethacrylate) graft copolymer. J. Hazard. Mater 2008;159(2–3):372–379. [PubMed: 18367330]

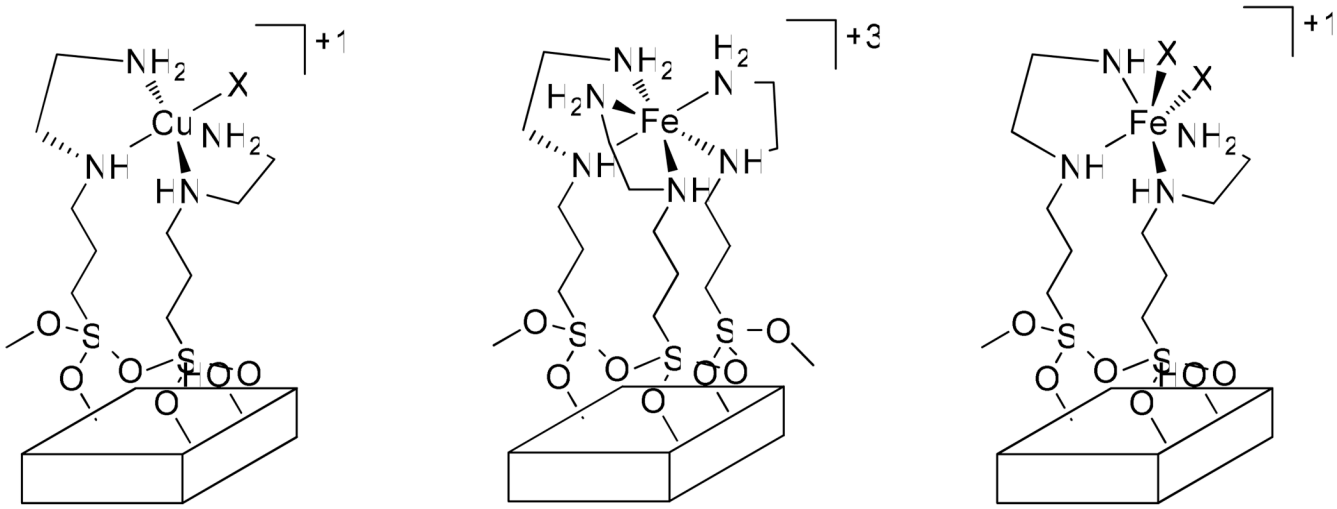


**FIGURE 1.**
Structure of the anion binding sites in Cu-EDA-SAMMS and Fe-EDA-SAMMS (1:3 Fe-EDA complex, center; 1:2 Fe-EDA complex, right).

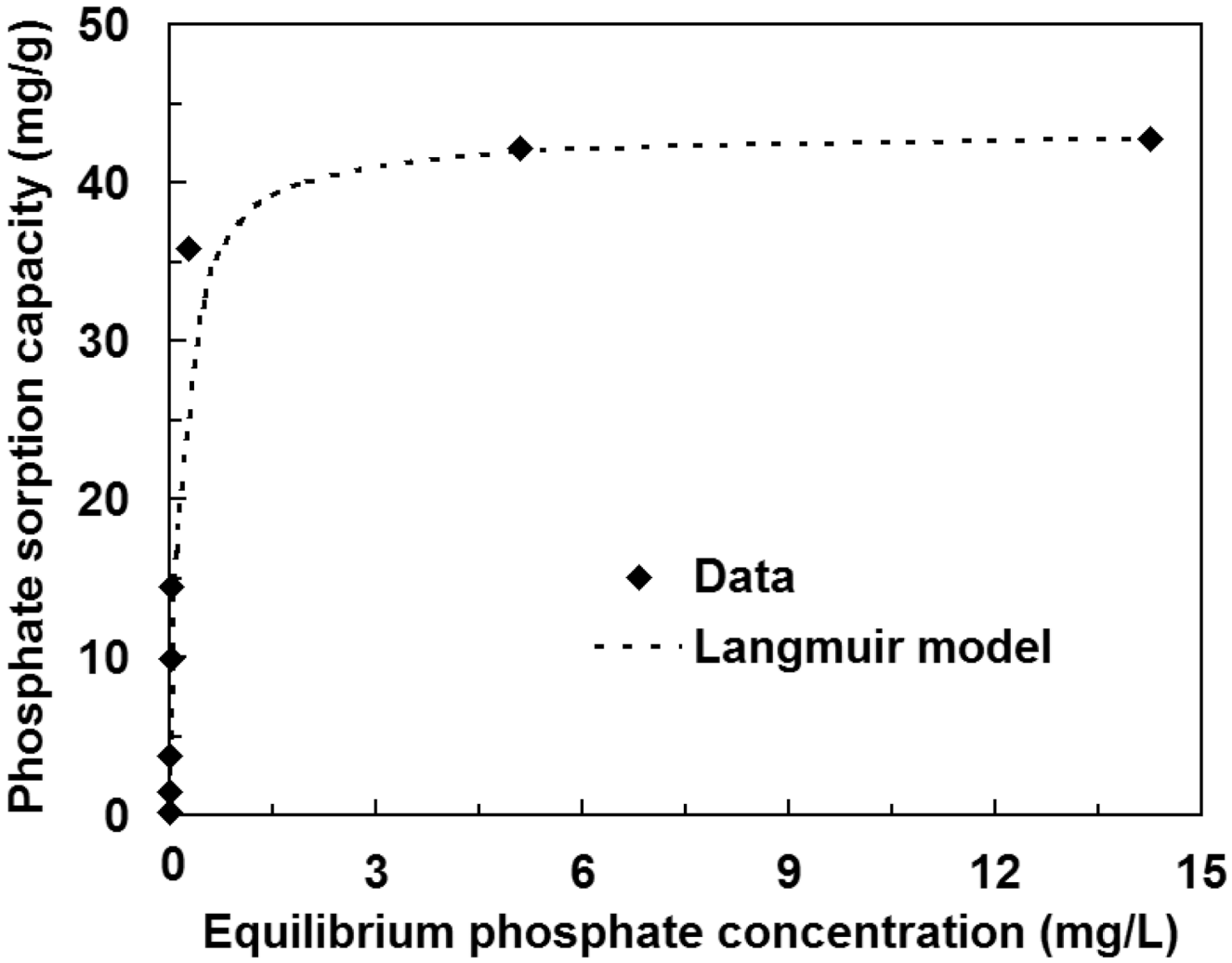


**FIGURE 2.**
Adsorption isotherm of phosphate on Fe-EDA-SAMMS in DI water (pH 5.0), L/S of 10,000 mL/g, symbols represent data, and dash-line represents Langmuir isotherm fitting.

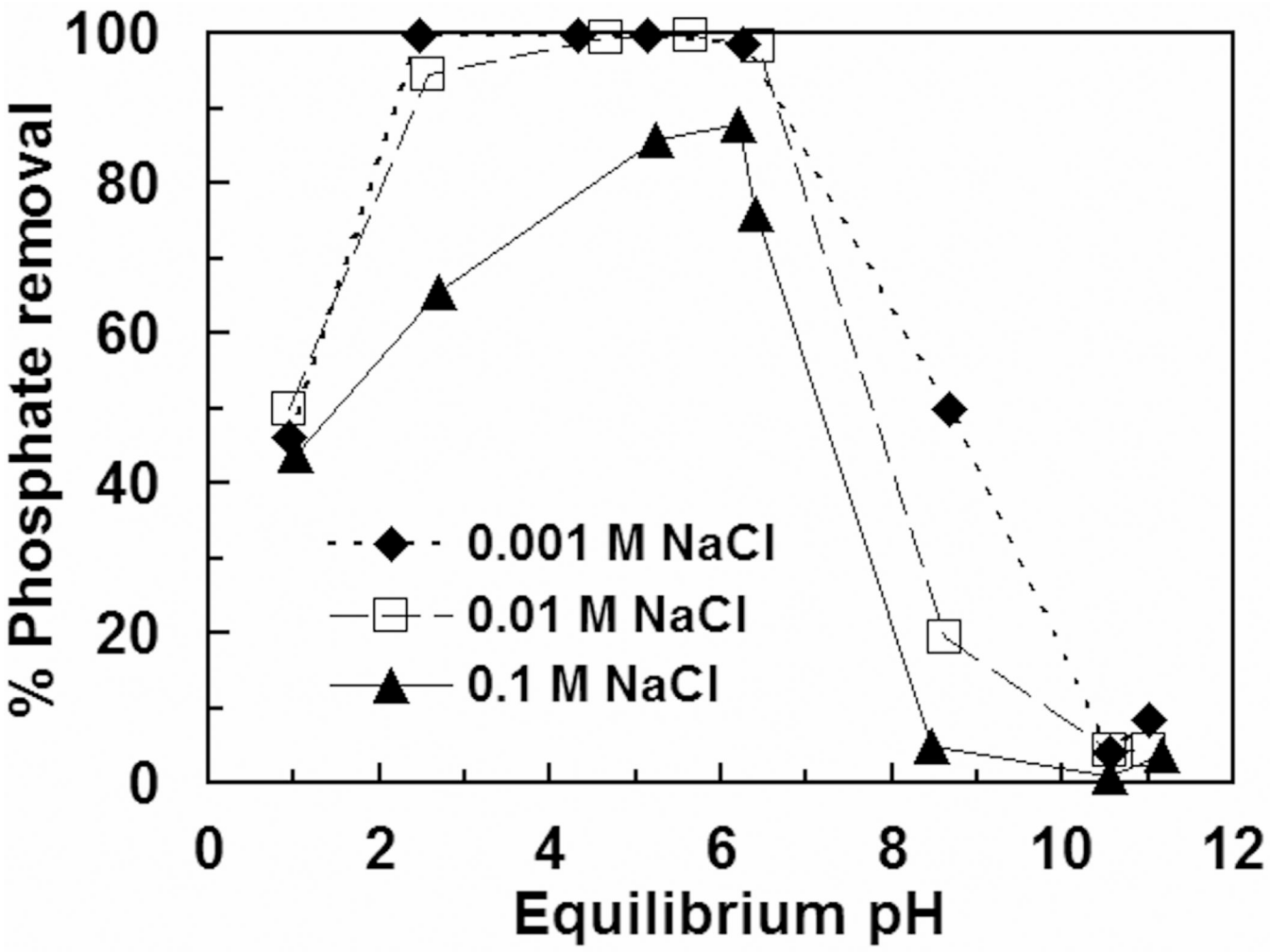


**FIGURE 3.**
Effects of pH and ionic strength on phosphate adsorption on Fe-EDA-SAMMS in DI water, initial phosphate concentration of ~2 ppm, L/S of 1000 mL/g.

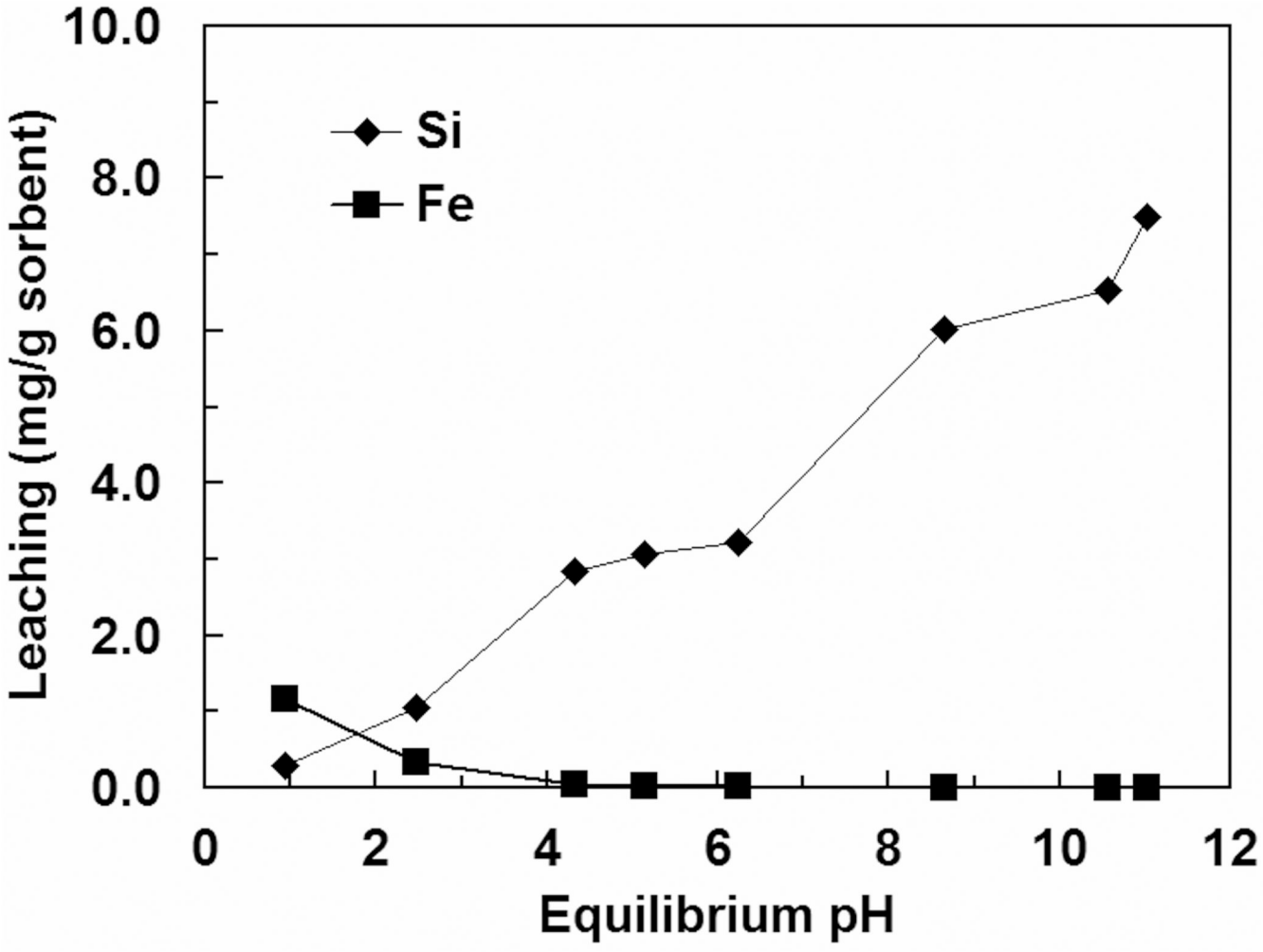


**FIGURE 4.**
Effect of pH on Si and metal cation (Fe) leaching from Fe-EDA-SAMMS in solutions containing 0.001 M NaCl, and ~2 ppm of phosphate, L/S of 1000 mL/g.

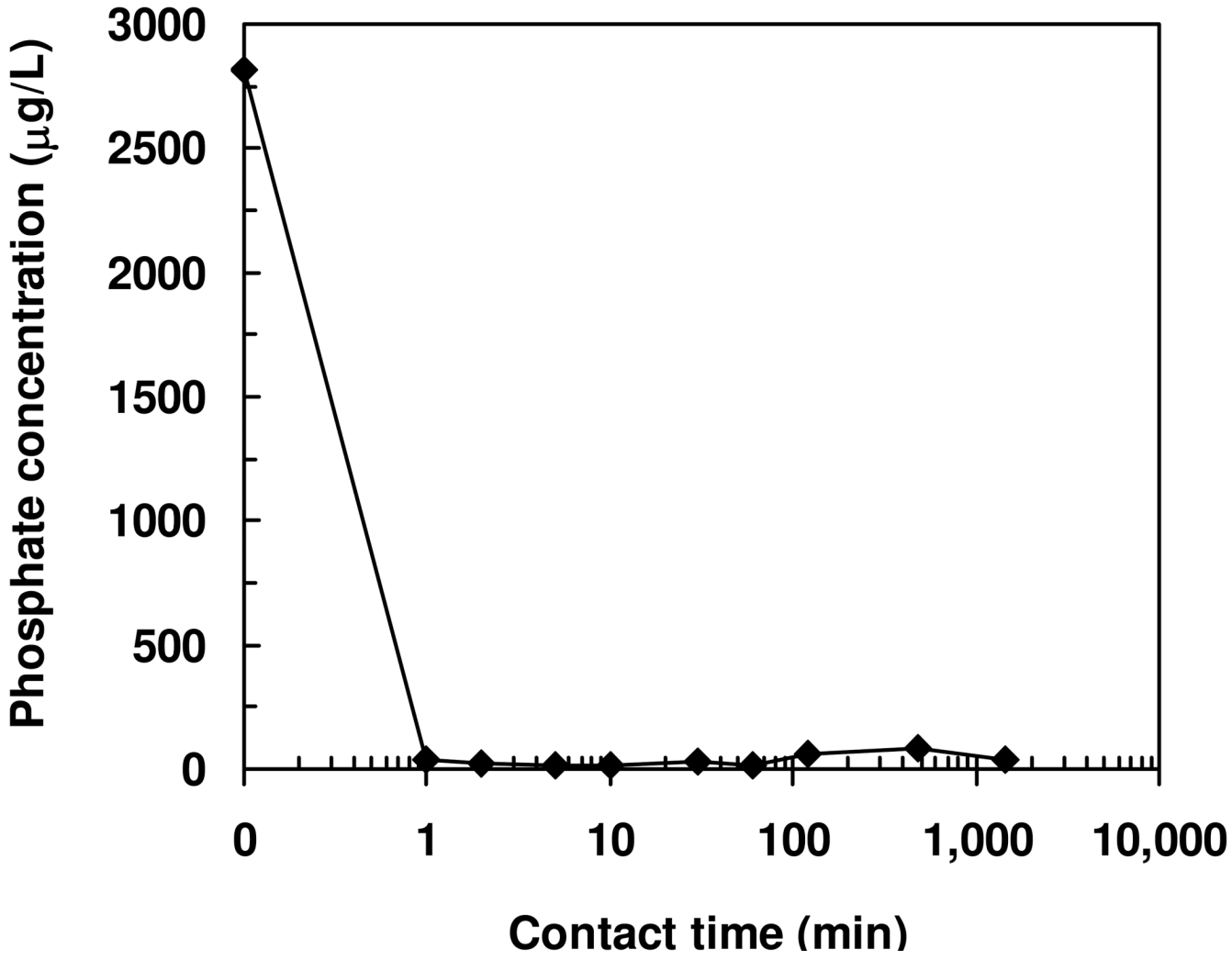


**FIGURE 5.**
Sorption kinetics of phosphate on Fe-EDA-SAMMS in DI water (pH 5.0), L/S of 1000 mL/g.

## TABLE 1

Distribution Coefficients ($K_d$, mL/g) of Phosphate Adsorption on Fe-EDA-SAMMS and Cu-EDA-SAMMS and the Leaching of Silica and Metal Cations.

| Sorbent | Final pH | $K_d$ (mL/g) | Silica (mg/g) | Metal cation (mg/g) |
|---|---|---|---|---|
| Fe-EDA-SAMMS | 4.6 | 310000 | 5.18 | 0.06 (Fe) |
| Cu-EDA-SAMMS | 5.8 | 110000 | 8.96 | 0.92 (Cu) |

Initial phosphate concentration of ~1 ppm, liquid-to-solid ratio (L/S) of 1000 mL/g

## TABLE 2

Effect of Coexisting Anions on Phosphate Removal by Fe-EDA-SAMMS

| Matrix | Final pH | % Phosphate removal |
|---|---|---|
| Phosphate | 4.6 | 99.7 |
| Phosphate + 0.01 M Sodium chloride | 5.7 | 99.6 |
| Phosphate + 0.01 M Sodium nitrate | 6.0 | 96.8 |
| Phosphate + 0.01 M Sodium bicarbonate | 8.1 | 80.2 |
| Phosphate + 0.01 M Sodium sulfate | 7.4 | 65.1 |
| Phosphate + 0.01 M Sodium citrate | 7.2 | 25.9 |

Initial phosphate concentration of ~1 ppm, L/S of 1000 mL/g